Effect of Chain Unsaturation on Polymethylene Lamellar Packing: Solid-State Structure of a Symmetric *trans*-Alkene

Douglas L. Dorset*

Electron Diffraction Department, Hauptman-Woodward Medical Research Institute, 73 High Street, Buffalo, New York 14203-1196

Robert G. Snyder

Chemistry Department, University of California, Berkeley, California 94720-1460

Received September 1, 1999; Revised Manuscript Received October 12, 1999

ABSTRACT: The orthorhombic crystal packing of 15-*trans*-triacontene was determined from electron diffraction intensities observed from epitaxially oriented and from solution-grown samples and by infrared spectroscopy of melt-crystallized thin layers. As determined from systematic absences in 0*kl* and *hhl* patterns, the pseudo-orthorhombic space group is *Aa* with cell constants $a = 7.48(3)$, $b = 4.99(3)$, and $c/2 = 39.8(1)$ Å. The structural conformation around the *trans* double bond is very similar to that found earlier for odd-chain polyalkenamers; i.e., the single bonds adjacent to the olefinic group have *skew* and anti-*skew* arrangements. Infrared spectra indicate that the formal molecular centrosymmetry around the double bond is not preserved by the chain conformation in the solid state. The chain layers stack in a way reminiscent of the B-polymorphic packing of odd-chain *n*-paraffins. In keeping with this chain jog, the olefin is completely insoluble in the solids containing the paraffin with the same carbon number, *n*-triacontane.

Introduction

Polydispersity provides a mechanism for controlling the physical properties of natural products containing linear chains. While the melting behavior of paraffin waxes and polyethylenes is strongly influenced by the distribution of saturated chain lengths in a solid solution, other factors such as chain branching and unsaturation can also be important. What is known quantitatively about the structural interactions of methyl, ketone, and hydroxyl branches and double-bond inclusion in polymethylene chain layer packing has been obtained from the crystal structures of the fatty acids.[1,2] However, virtually all the quantitative crystallographic investigations[3] of olefinic chains in fatty acids have examined the *cis* chain configuration. The single *trans*-unsaturated fatty acid investigated[4] has been a rather poorly defined projected structure of a natural product isolated from plant seeds.

Olefins can appear with *n*-alkanes in certain crude petroleum fractions[5] although they are only infrequently components of solidified waxes.[6] While it is already known that a *cis* double bond in a polymethylene chain, when comixed with an *n*-alkane of the same chain length, will lead to a fractionation of components,[2] there is no similar appraisal of what happens when the conformation is *trans*. Fatty acid chains containing *cis* or *trans* double bonds can produce similar overall chain conformation in solid cholesteryl esters.[7] However, this says nothing about the case when all chains themselves are densely copacked, via a methylene subcell, in a layer instead of the rather loose constraints found for these unsaturated ester chains in the so-called monolayer I polymorphic form. The only information available, apparently, is for the polyalkenamers[8] where the saturated polymethylene chain segment adjacent to the double bond is rather short.

* To whom correspondence should be addressed.

The basic question is, therefore, one of overall chain conformation. Can the *trans* double bond be accommodated into an overall plane of methylene groups, or does the conformational freedom near the double bond always impose a jog in the chain? Are the *trans*-olefins therefore cosoluble with similar chain length *n*-alkanes in the solid state?

Material and Methods

Olefin and Its Crystallization. A sample of 15-*trans*-triacontene, *n*-$C_{30}H_{60}$, was obtained privately as a gift from Proctor and Gamble Inc. and was stated to be 99.96% pure. As received, the material comprised colorless thin crystalline plates. For DSC measurements (see below), the samples were evaluated without further recrystallization.

Microcrystals of the olefin were prepared in two ways. Thin lozenge crystals in a projection down [001] were obtained by evaporation of dilute solutions in light petroleum onto a carbon-film-covered electron microscope grid. As observed by bright field electron microscopy, the boundary faces are (001), the major face, and {110}, as found for the *n*-paraffins. However, there is also a well-defined (100) face sometimes seen also for polyethylene[9] (Figure 1a).

Epitaxial orientation was obtained on benzoic acid, adapting the procedure of Wittman, Hodge, and Lotz.[10] After a mica sheet was cleaved, the dilute solution in light petroleum was evaporated to leave the olefin solid. Carbon-film-covered electron microscope grids were then placed face down on this solid and an excess of benzoic acid crystals distributed over the surface. The second mica sheet face was placed over this physical mixture to make a sandwich. This sandwich was then placed on a thermal gradient, first comelting the organic materials and then recrystallizing them by sliding the sandwich to a cooler part of the aluminum bar spanning a hot plate and thermoelectric cold plate. Epitaxial orientation occurred at the interface between the chain molecule and the benzoic acid nucleator, as explained by a eutectic binary phase diagram.[11] The sandwich was then opened to expose the grids with organic mass on their surfaces and the benzoic acid then removed by sublimation overnight in vacuo. (After sublimation

10.1021/ma991505g CCC: $18.00
Published on Web 11/10/1999

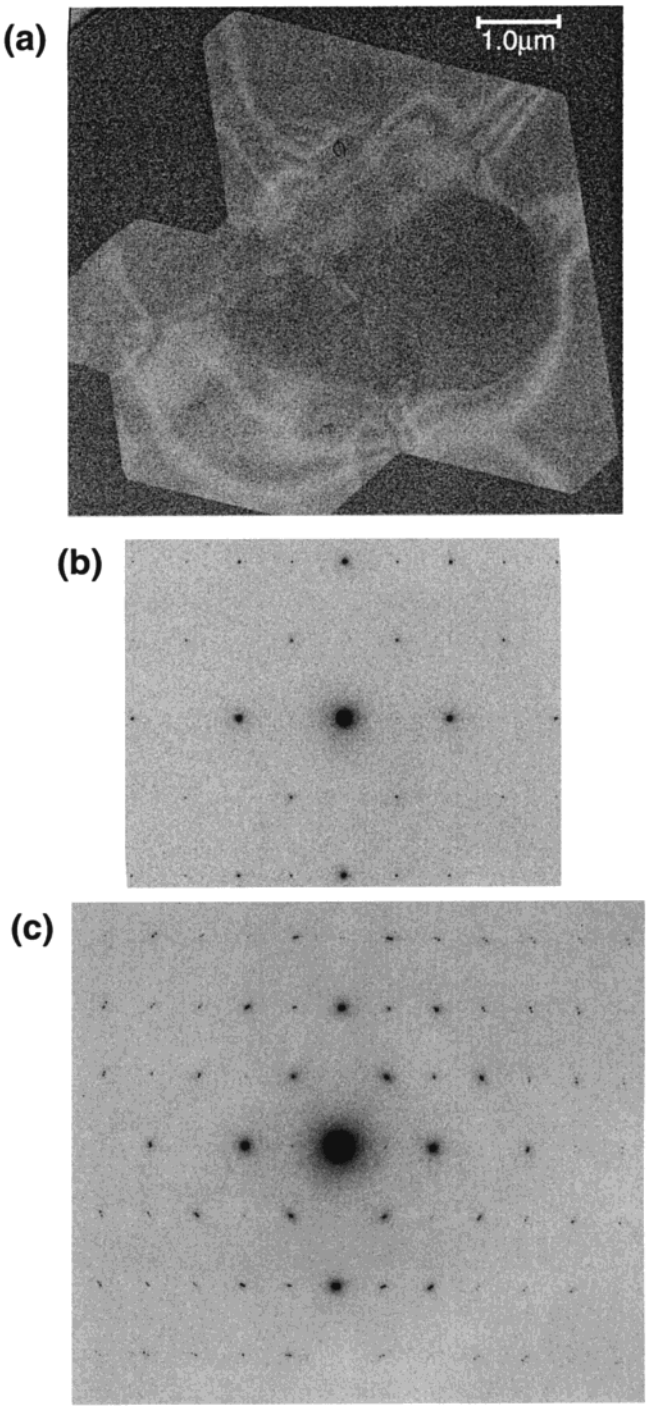

Figure 1. (a) Lozenge habit for a crystal of 15-*trans*-triacontene grown from light petroleum. A truncation at the (100) face is observed in addition to the usual {110} boundaries found for the orthorhombic paraffins. (b) Electron diffraction pattern from (a) using a ca. 0.7 μm diameter selected area aperture. (c) Electron diffraction pattern in the same projection using a ca. 2.9 μm diameter aperture.

of the benzoic acid, the oriented olefin crystals lay on the undamaged carbon film of the electron microscope grid.)

Differential Scanning Calorimetry. DSC measurements were made on 0.50−2.00 mg samples with a Mettler TA 3300 instrument. Scans were made at 5°/min over the range from 0 to 100 °C at the highest sensitivity setting for the glass sensor. The transition enthalpies were calibrated against an indium standard and the temperature scale against known transitions for 18 *n*-alkanes and *n*-perdeuterioalkanes.[2,12] For example, the determined premelt and melting transitions for *n*-triacontane were 62.0 °C (62.0 °C) and 65.5 °C (65.8 °C), respectively (where the literature values[2] are in parentheses). The melting point for 15-*trans*-triacontene was found to be 54.5 °C, and $\Delta H_m = 25.4$ kcal/mol.

In one series of experiments, the thermal behavior of various concentrations of the olefin with *n*-triacontane (Fluka, > 99% pure) was investigated. Samples were weighed on an analytical balance into aluminum pans. After sealing these, they were first heated to 100 °C to cosolubilize the components in the melt and then cooled to 0 °C to begin the heating scan.

Electron Microscopy/Diffraction. All electron diffraction experiments were carried out at 100 kV on a JEOL JEM-100CX II electron microscope equipped with a side entry eucentric goniometer stage. For some experiments, seeking *hhl* diffraction patterns from epitaxially oriented samples at 33° tilt of the stage, a Gatan 650 rotation holder was employed to orient the unit cell *c** axis parallel to the goniometer tilt axis. All selected area experiments were carried out using usual low-dose conditions, minimizing radiation damage to the specimens.[13] The selected area used for the experiment typically had a 2.9 μm diameter although a 0.7 μm diameter was also employed in a test of the *hk*0 diffraction from solution-crystallized lozenges. Diffraction spacings were calibrated against a gold powder standard, using a thin layer of the noble metal deposited on one part of a specimen grid in a vacuum coater unit.

Bright field electron micrographs were obtained from solution-grown samples at 10K× magnification. Following the usual procedure,[13] an aperture selected the central spot of the diffraction pattern to provide image contrast. These exposures also were made on the same CEA Reflex X-ray film used for the diffraction studies.

Data Reduction and Crystal Structure Analysis. Intensities of diffraction spots were measured from the films using a Joyce-Loebl Mk. III C flat-bed microdensitometer. Many diffraction patterns were obtained from a single projection to test the self-consistency of the data, as explained in a recent paper.[14] Because of the large relative elastic bend of these crystalline samples within the selected areas, no Lorentz correction was applied to the intensities.[13] For combining the 0*kl* and *hhl* data sets, the intensity summation of the common 00*l* row was used for scaling one to the other.

An initial analysis of the layer structure was made by evaluation of the 00*l* row of reflections assuming the symmetry to be approximately $P\bar{1}$. An overall phase value of π radians was applied to the inner order 00*l* reflections, in accord with a paraffin model. The phase value of the (00 58) reflection was assumed to be 0 rad, and algebraic phase values were given to (00 60), (00 62), and (00 64). After calculating the one-dimensional Fourier transform after phase permutation, solutions were sought that would contain 30 carbon positions. As will be explained below, this initial result justified construction of three-dimensional models.

Infrared Spectroscopy. Infrared measurements were carried out on thin-layer samples cooled from the melt between two KBr windows. Measurements were made at room temperature with an evacuatable Nicolet model 8000 FTIR spectrometer equipped with a cooled MCT/B detector. Operating parameters were chosen to provide a resolution of 1.0 cm^{-1}. Band assignments made in previous studies[15] were used as the spectrum of the *trans*-alkene was compared to that of the corresponding even-chain *n*-alkane (*n*-triacontane), as well as a neighboring odd-chain *n*-alkane (*n*-nonacosane). Of particular interest were the CH_2 scissors band near 1475 cm^{-1}, the CH_2 rocking bands near 720 cm^{-1}, the alkene group C−H stretching bands near 3000 cm^{-1}, and the symmetric methyl group bending mode ("umbrella band") near 1370 cm^{-1}. Other bands, where conformation disorder is manifested,[16] were also consulted during these studies.

Results

It is clear that the layer packing of the chain is rectangular (untilted) in the orthorhombic perpendicular ($O_\perp$) methylene subcell. Electron diffraction patterns from the lozenge crystals (Figure 1a) are characteristic

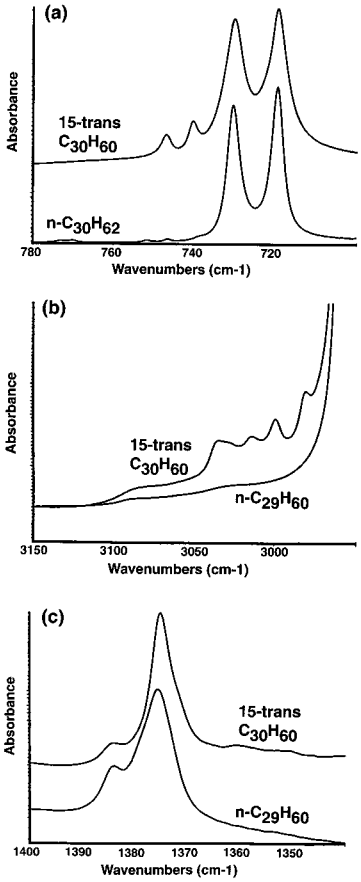

Figure 2. Infrared spectra of 15-*trans*-triacontene compared to *n*-alkanes. (a) Methylene rocking bands near 720 cm^{-1}. (b) C−H stretching modes for the double-bond moiety near 3000 cm^{-1} showing four bands not seen for the paraffin *n*-$C_{29}H_{60}$. (c) Umbrella bands for the *trans*-alkene compared to those of *n*-$C_{29}H_{60}$.

of this subcell (Figure 1c), especially from the measured unit cell spacings (see below). Moreover, the shape of the 720 cm^{-1} rocking band (Figure 2a) is very similar to that of the orthorhombic *n*-alkanes, with very little difference found in the band splitting (10.7 cm^{-1} vs 10.5 cm^{-1}). The characteristic splitting of the CH_2 scissors band is also similar to that of the orthorhombic alkanes.

At first glance (Figure 3), the 0*kl* diffraction patterns from the epitaxially oriented *trans*-olefin appear to be very similar to the ones obtained from an orthorhombic *n*-paraffin. Closer inspection, however, reveals some differences. First, the *l*-indices of the major 01*l* reflections are 29, 31, and 33, respectively, violating the rule[13] that there should be a simple relationship ($l = m$, $m + 2$) between this index and the carbon length, m, of the chain C_mH_{2m}. However, for this molecule, $m = 30$, not 31. In the 0*kl* pattern, as well as the *hhl* pattern, the systematic absences for reflections occur at $k + l = 2n + 1$, which is inconsistent with the index rule expected for an even-chain orthorhombic paraffin in space group $Pca2_1$. The indices of observed reflections are, however, in accord with space group Aa (or $A2_1am$) proposed for the B-polymorph of odd-chain paraffins,[17] expressed when these paraffins are crystallized from the melt or when the solution-crystallized A-form is heated. Nevertheless, the measured lamellar layer spacing $c/2 = 39.8(1)$ Å is also very close to the value predicted[18] for the even-chain paraffin with 30 carbons, *n*-triacontane, i.e., 39.9 Å.

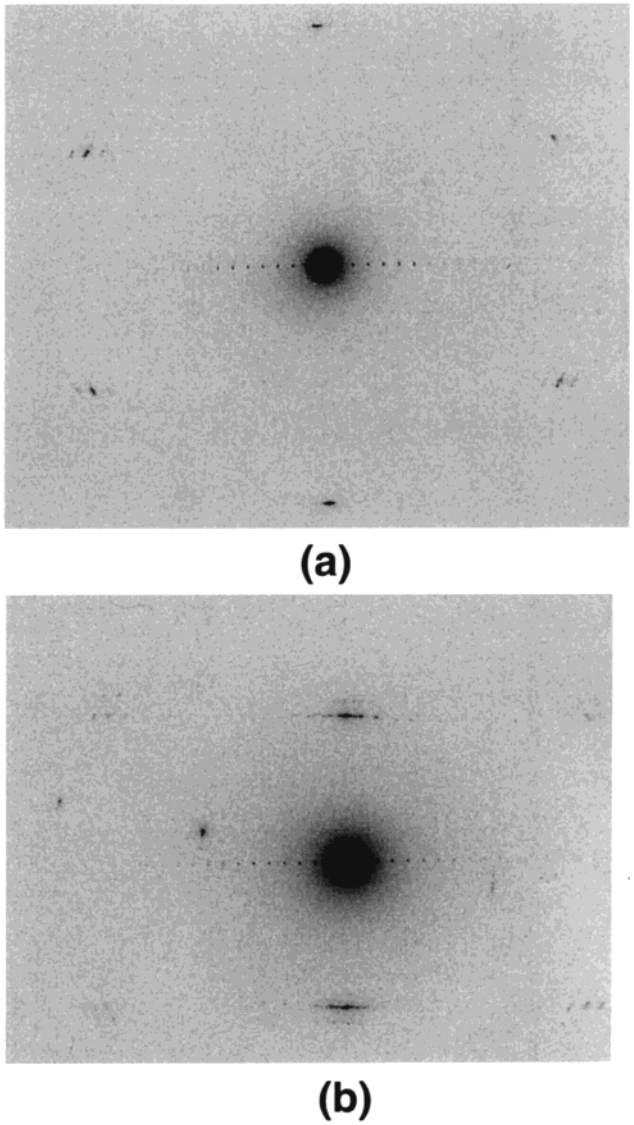

Figure 3. Electron diffraction patterns from epitaxially oriented alkene samples. (a) 0*kl* pattern (0° tilt); (b) *hhl* pattern (33° tilt around *c**).

Electron diffraction patterns from multilamellae grown from solution (Figure 1c) also have an unusual feature. The average spacings are in accord with those of all orthorhombic *n*-paraffins, i.e., $a = 7.48(3)$ and $b = 4.99(3)$ Å. However, the reflections in rows where $k = 2n + 1$ are rather weak compared to the other ones. Patterns obtained at smaller selected areas (Figure 1b) emphasize this difference. For example, $\sum|F_{h10}|/\sum|F_{h00}|$ changes from 0.73 to 0.51 when the selected area diameter is changed from 2.9 to 0.7 μm whereas the respective change in $\sum|F_{h20}|/\sum|F_{h00}|$ is only 1.36−1.28. Because of the diffraction incoherence induced by an elastic crystal bend (seen as contours in Figure 1a) in projections down a long unit cell axis,[19] this indicates that the reciprocal lattice rows in the *hk*0 pattern, where $k = 2n + 1$, may be extinct for flat crystals, also in accord with space group Aa. Starting with the intensities from an *hk*0 pattern from such a multilayer, and assigning the phases expected for the polyethylene structure in this projection, additional chain sites are indicated in ensuing Fourier refinement (Figure 4) at chain mass centers consistent for the Aa layer stacking (with details distorted by imposition of the $Pnam$ space group of the infinite polymer[20]).

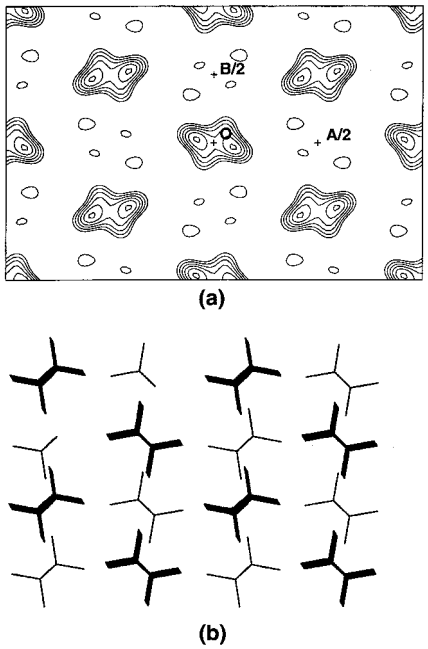

Figure 4. (a) Structure refinement of the layer structure with *hk*0 electron diffraction intensity data as in Figure 1c, starting with a polyethylene layer model. Although the space group is not the same as found for the *trans*-alkene, the refinement indicates that the next layer of chains will pack with ends at the gaps left by the previous layer. (b) The packing of orthorhombic odd-chain paraffins in the B-polymorph which has the same displacement of layers as in (a).

Vibrational spectroscopy supports this layer stacking model. Comparing the methyl group bending frequencies for the *trans*-alkene to those from *n*-$C_{29}H_{60}$ crystallized from the melt (B-polymorph), there is little difference in the spectra. This band is very sensitive to the type of layer stacking sequence. In addition, there is no evidence of bands associated with conformational disorder[16] for either the alkane or olefin.

Initially it was not easy to compromise an even-chain structure with a space group symmetry expected for odd-chain alkanes, especially if all of the bond conformations were expected to be close to 180°. This would require that the methyl group interactions of even-chain layers would mimic those expected for the higher-energy odd-chain paraffin polymorph in space group *Aa*. Energetically, this packing would be extremely unlikely since the protruding terminal methyl groups point in the wrong direction. After a few trials based on an average C31 layer structure, involving translational displacements of C30 chain segments, it was decided that a completely straight-chain model was not a realistic option.

The dissimilarity between the two crystal packing arrays, i.e., for olefin and alkane, respectively, was, in fact, disclosed by the binary phase diagram of 15-*trans*-triacontene with *n*-triacontane. This construction from calorimetric experiments can be viewed as an independent, sensitive probe of relative molecular volumes, a device often employed by Kitaigorodskii.[21] As shown by the eutectic relationship in Figure 5, the two molecules are completely insoluble, so they cannot have the same molecular conformation or crystal structure. The methylene scissors band measurements in infrared spectra also indicated that, while there are no *cis*-conformations anywhere in the chain, the conformation of the methylene carbons adjacent to the *trans*-double bond should be somewhat different from that of the rest of the chain.

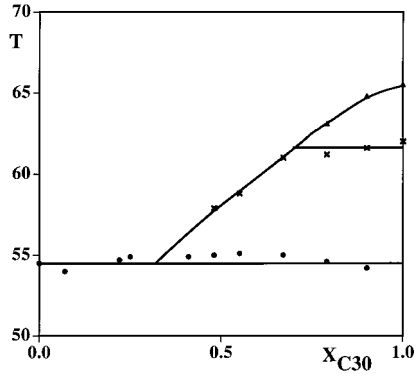

Figure 5. Binary phase diagram of 15-*trans*-triacontene with *n*-triacontane.

Table 1. Carbon Coordinates for 15-*trans*-Triacontene in Space Group *Aa*

x/*a*	*y*/*b*	*z*/*c*	*x*/*a*	*y*/*b*	*z*/*c*
0.043	0.175	0.0184	0.117	0.328	0.2540
−0.035	0.308	0.0344	0.191	0.196	0.2700
0.043	0.175	0.0504	0.113	0.325	0.2860
−0.035	0.308	0.0664	0.191	0.192	0.3014
0.043	0.175	0.0824	0.113	0.325	0.3180
−0.035	0.308	0.0984	0.191	0.192	0.3340
0.043	0.175	0.1144	0.113	0.325	0.3500
−0.035	0.308	0.1304	0.191	0.192	0.3660
0.043	0.175	0.1464	0.113	0.325	0.3820
−0.035	0.308	0.1630	0.191	0.192	0.3980
0.043	0.175	0.1784	0.113	0.325	0.4140
−0.035	0.308	0.1944	0.191	0.192	0.4300
0.043	0.175	0.2097	0.113	0.325	0.4460
−0.035	0.304	0.2264	0.191	0.192	0.4620
0.039	0.172	0.2424	0.113	0.325	0.4780

A solution to the molecular packing problem was suggested by the earlier analysis of *trans*-polyalkenamers by Natta et al.[8] The odd-chain polymer structures pack with similar lateral unit cell dimensions to the orthorhombic paraffins and yet contain chains that incorporate a jog around the double bond so that there are actually two collinear segments of the entire chain. From this work, it was also seen that the [100] view would be the worst possible one for discerning any structural difference from the saturated *n*-alkanes. The jog in the chain is not apparent in this projection. A chain crankshaft model (coordinates in Table 1) was constructed, therefore, on the basis of the polymer conformation around the double bond[8] and then packed in space group *Aa*. Testing against 56 0*kl* and *hhl* amplitudes, the overall fit of carbon positions was $R = 0.27$ when an isotropic $B = 6.0$ Å^2 was applied to these atoms (Table 2). (Consistent with findings for pure *n*-paraffins grown from the melt, some disorder (fractional occupancy) was built into the final methyl group position during the crystal structure analysis, even though conformational disorder was not especially noticed in the infrared spectra.) The *skew* bond conformational angle next to the double bond, 125°, was assumed to be compensated by its negative value on the other side. All other conformations were near 180°, and bond distances and angles were defined to be close to the values expected for similar materials. The observed *hk*0 amplitudes from multilamellar crystals were also compared to the three-dimensional model; the agreement was poor ($R = 0.62$) if a flat crystal model was assumed. If a compensation is made for even a slight amount (e.g., 1°) of overall elastic crystal bend, the agreement greatly improved ($R = 0.29$) as shown in

Table 2. Observed and Calculated Structure Factor Magnitudes for the Crystal Packing Model in Table 1

hkl	$\|F_{obs}\|$	$\|F_{calc}\|$	*hkl*	$\|F_{obs}\|$	$\|F_{calc}\|$	*hkl*	$\|F_{obs}\|$	$\|F_{calc}\|$
00 2	1.48	1.46	00 40	0.10	0.06	02 4	0.39	0.36
00 4	1.28	1.09	00 42	0.13	0.20	02 60	0.68	0.36
00 6	0.97	1.28	00 44	0.10	0.06	02 62	0.59	0.22
00 8	0.92	0.89	00 46	0.14	0.18	02 64	0.70	0.48
00 10	0.85	0.95	00 48	0.10	0.11	03 29	0.53	0.57
00 12	0.80	0.56	00 50	0.12	0.12	03 31	1.27	1.58
00 14	0.74	0.66	00 52	0.10	0.17	03 33	0.74	0.94
00 16	0.72	0.22	00 54	0.24	0.04	04 0	0.70	0.15
00 18	0.68	0.38	00 56	0.20	0.30	11 1	3.63	3.45
00 20	0.53	0.04	00 58	0.28	0.05	11 3	2.70	3.18
00 22	0.51	0.22	00 60	0.92	0.84	11 5	0.80	0.78
00 24	0.42	0.16	00 62	0.80	0.52	11 29	0.80	0.18
00 26	0.42	0.15	00 64	1.01	1.12	11 31	1.01	1.17
00 28	0.26	0.14	01 27	0.29	0.03	11 33	0.80	0.29
00 30	0.37	0.05	01 29	0.91	0.75	11 63	0.91	1.11
00 32	0.17	0.00	01 31	2.53	2.07	22 0	1.54	1.74
00 34	0.38	0.06	01 33	1.32	1.20	22 2	1.00	1.59
00 36	0.10	0.04	02 0	4.43	4.70	22 4	0.59	0.16
00 38	0.30	0.19	02 2	0.54	0.43			

Table 3. Correction of Calculated *hk*0 Diffraction Data for Elastic Crystal Bending (1°)

*hk*0	$\|F_{bend}\|$	$\|F_{obs}\|$	*hk*0	$\|F_{bend}\|$	$\|F_{obs}\|$
200	3.16	2.78	320	0.31	0.49
400	0.47	1.12	420	0.32	0.38
600	0.11	0.21	520	0.74	0.40
110[a]	1.71	1.52	620	0.08	0.32
210[a]	0.22	0.50	130[a]	0.40	0.93
310[a]	0.73	0.84	230[a]	0.44	0.60
410[a]	0.38	0.53	330[a]	0.20	0.39
510[a]	0.33	0.64	430[a]	0.60	0.48
610[a]	0.39	0.41	040	0.14	0.22
020	2.60	2.37	140	0.24	0.31
120	0.42	0.70	240	0.17	0.40
220	1.10	1.05	340	0.28	0.60

[a] Systematically absent in space group *Aa*.

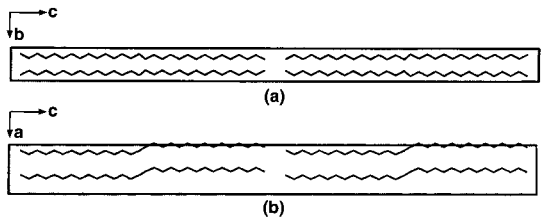

Figure 6. Packing model for 15-*trans*-triacontene. (a) [100] projection; (b) [010] projection.

Table 3. The overall packing model is shown in Figure 6.

The symmetric conformation was not supported by infrared measurements, however. Formally, the *trans*-alkene would be centrosymmetric. The olefinic C−H stretching modes in the vicinity of 3000 cm^{-1} should produce one IR-active band for an isolated molecule or two in the layer subcell with two molecular chains (e.g., $O_\perp$) if this molecular centrosymmetry were to be preserved in the crystal structure. Instead, four bands were observed (Figure 2b), implying that the molecular inversion center is not retained in the crystal.

Discussion

This structure analysis of a *trans*-alkene, based on electron diffraction and infrared spectroscopy, shows, first of all, that the molecular conformation is consistent with that found for a linear polyalkenamer,[8] where the twisted chains are closely packed in a rectangular layer. It is also similar to the conformation found for the *trans*-unsaturated cholesteryl ester[7] where the chains are not confined to a close-packed layer. It has been shown[22] that the barrier to rotation about single bonds adjacent to double bonds is somewhat lower than that for the saturated *n*-alkanes. From this study it is clear that the summed van der Waals packing forces in a rectangular layer for a very long polymethylene segment are not sufficient to overcome a preferred nonplanar conformation near the *trans* double bond. When an unsaturated bond is placed in the center of the chain, therefore, the olefins cannot be cosolubilized with saturated paraffins. Hence, the energetic change resulting from a favorable nonplanar conformation is greater than can be compensated by an entropic mixing of an *all-trans*-alkene in a putative solid solution with the alkane.[23]

There is a question, however, about the identity of *skew* (+α) and anti-*skew* (−α) conformational angle magnitudes on either side of the *trans* double bond assumed in this structure analysis. Least-squares refinement against fiber X-ray data from the polyalkenamers[8] supported the identity of these values. This identity was also assumed (but not proved) for the crystal structure of elaidic acid.[24] This identity was not found for cholesteryl palmitelaidate,[7] where the two angles are 113° and −124°, respectively, but again, these cholesteryl ester chains do not pack with a polymethylene subcell. Breakdown of inversion symmetry around the double bond, indicated by infrared spectra, on the other hand, points to a nonequivalence of these angles in the close-packed *trans*-alkene structure. This is somewhat surprising, since molecular inversion centers should be preserved by space group symmetry.[25] However, the current model packs a formally centrosymmetric molecule into a noncentrosymmetric space group so that this symmetry preservation is not required, similar to the case of the orthorhombic even-chain *n*-paraffins.[26] A chain packing incorporating the Cho and Craven[7] conformational sequence gives only a slightly worse crystallographic residual ($R = 0.31$) than the model in Table 1, but the difference may not be significant, especially since there are too few observed diffraction intensity data to attempt a further refinement or to perform statistically meaningful tests of the models. Indeed, the cholesteryl ester crystal structure implies that the centrosymmetric *skew*, anti-*skew* conformation may not be energetically favorable for a free chain.

Certainly further work is needed for this compound to define its crystal structure to greater accuracy. While the epitaxial orientation of the chains was sufficient to obtain relevant single-crystal electron diffraction data, the most easily expressed [100] zonal projection was one that was not very sensitive to details of the molecular model. The [110] and [001] projections merely provided supportive justification for the structure with relatively few additional unique data. Spectroscopic measurements and construction of the binary phase diagram were extremely important for this analysis to indicate possible differences in molecular conformation from the initial centrosymmetric model used in the crystal structure analysis. The appearance of a well-defined [100] crystal face also indicates different preferred growth interactions, e.g., in a "periodic bond" model[27] (where the "bonds" are preferred pairwise vectorial interactions between neighboring molecules), somewhat different from the corresponding *n*-alkane. This difference may also be an important consequence of the molecular jog,

since this deviation from planarity of the whole chain is largely expressed along the unit cell *a*-axis. Attempts will be made to crystallize this material slowly from a solvent with a low vapor pressure to obtain samples sufficient for X-ray data collection.

Acknowledgment. Research was supported by a grant from the National Science Foundation (CHE-9730317) to HWI and from the National Institutes of Health (GM-27690) to U. C. Berkeley, which are gratefully acknowledged. We thank Dr. Dolores Clavell-Grunbaum for obtaining the infrared spectra from the olefin and *n*-paraffins.

References and Notes

(1) Sydow, E. von *Ark. Kemi* **1956**, *9*, 231. Abrahamsson, S. *Ark. Kemi* **1959**, *14*, 65. Sato, K. *Prog. Colloid Polym. Sci.* **1998**, *108*, 58.
(2) Small, D. M. *The Physical Chemistry of Lipids. From Alkanes to Phospholipids*; Plenum: New York, 1986; pp 107ff, 228−229, 256ff.
(3) Abrahamsson, S.; Ryderstedt-Nahringbauer, I. *Acta Crystallogr.* **1962**, *15*, 1261. Ernst, J.; Sheldrick, W. S.; Führhop, J. H. *Z. Naturforsch.* **1979**, *34B*, 706. Kaneko, F.; Yamazaki, K.; Kitagawa, K.; Kikyo, T.; Kobayashi, M.; Kitagawa, Y.; Matsuura, Y.; Sato, K.; Suzuki, M. *J. Phys. Chem.* **1997**, *B101*, 1803. Kaneko, F.; Kobayashi, M.; Kitagawa, Y.; Matsuura, Y.; Sato, K.; Suzuki, M. *Acta Crystallogr.* **1992**, *C48*, 1060. Kaneko, F.; Kobayashi, M.; Kitagawa, Y.; Matsuura, Y.; Sato, K.; Suzuki, M. *Acta Crystallogr.* **1992**, *C48*, 1057. Kaneko, F.; Kobayashi, M.; Kitagawa, Y.; Matsuura, Y.; Sato, K.; Suzuki., M. *Acta Crystallogr.* **1992**, *C48*, 1054.
(4) Tesche, O. A. *Acta Crystallogr.* **1954**, *7*, 737.
(5) Kinghorn, R. R. F. *An Introduction to the Physics and Chemistry of Petroleum*; Wiley: Chichester, England, 1983; pp 69ff.
(6) Warth, A. H. *The Chemistry and Technology of Waxes*; Reinhold: New York, 1947.
(7) Cho, S. I.; Craven, B. M. *J. Lipid Res.* **1987**, *28*, 80.
(8) Natta, G.; Bassi, I. W.; Fagherazzi, G. *Eur. Polym. J.* **1969**, *5*, 239.
(9) Bassett, D. C.; Keller, A. *Philos. Mag.* **1961**, *6*, 345.
(10) Wittmann, J. C.; Hodge, A. M.; Lotz, B. *J. Polym. Sci., Polym. Phys. Ed.* **1983**, *21*, 2495.
(11) Dorset, D. L.; Hanlon, J.; Karet, G. *Macromolecules* **1989**, *22*, 2169.
(12) Dorset, D. L.; Strauss, H. L.; Snyder, R. G. *J. Phys. Chem.* **1991**, *95*, 938.
(13) Dorset, D. L. *Structural Electron Crystallography*; Plenum: New York, 1995.
(14) Dorset, D. L.; McCourt, M. P.; Li, G.; Voigt-Martin, I. G. *J. Appl. Crystallogr.* **1998**, *31*, 544.
(15) Snyder, R. G. *J. Mol. Spectrosc.* **1961**, *7*, 116.
(16) Maroncelli, M.; Qi, S. P.; Strauss, H. L.; Snyder, R. G. *J. Am. Chem. Soc.* **1982**, *104*, 6237.
(17) Piesczek, W.; Strobl, G. R.; Malzahn, K. *Acta Crystallogr.* **1974**, *B30*, 1278.
(18) Nyburg, S. C.; Potworowski, J. A. *Acta Crystallogr.* **1973**, *B29*, 347.
(19) Cowley, J. M. *Acta Crystallogr.* **1961**, *14*, 920. Dorset, D. L. *Acta Crystallogr.* **1980**, *A36*, 592.
(20) Bunn, C. W. *Trans. Faraday Soc.* **1939**, *35*, 482. Abrahamsson, S.; Dahlen, B.; Löfgren, H.; Pascher, I. *Prog. Chem. Fats Other Lipids* **1978**, *16*, 125.
(21) Kitaigorodsky, A. I. *Mixed Crystals*; Springer-Verlag: Berlin, 1984.
(22) Nyburg, S. C. *X-ray Analysis of Organic Crystal Structures*; Academic: New York, 1961; p 169.
(23) Kitaigorodskii, A. I.; Myasnikova, R. M. *Sov. Phys. Crystallogr.* **1960**, *5*, 610.
(24) Ueno, S.; Suetake, T.; Yano, J.; Suzuki, M.; Sato, K. *Chem. Phys. Lipids* **1994**, *72*, 27. Kaneko, F.; Yano, J.; Sato, K. *Current Opinion Struct. Biol.* **1998**, *8*, 447.
(25) Kitaigorodskii, A. I. *Organic Chemical Crystallography*; Consultants Bureau: New York, 1961, p 104. Kitaigorodskii, A. I. *Sov. Phys. Crystallogr.* **1957**, *2*, 454.
(26) Teare, P. W. *Acta Crystallogr.* **1959**, *12*, 294.
(27) Bennema, P.; Liu, X. Y.; Lewtas, K.; Tack, R. D.; Rijpkema, J. J. M.; Roberts, K. J. *J. Cryst. Growth* **1992**, *121*, 679.

MA991505G